



# Stratification and mixed layer depth around Iceland: Characterization and inter-annual variability

Angel Ruiz-Angulo<sup>1</sup>, Esther Portela<sup>2</sup>, Charly de Marez<sup>1,2</sup>, Andreas Macrander<sup>3</sup>, Sólveig Rósa Ólafsdóttir<sup>3</sup>, Thomas Meunier<sup>4</sup>, Steingrímur Jónsson<sup>3,5</sup>, and M. Dolores Pérez-Hernández<sup>6</sup>

<sup>1</sup>Earth Science Institute, University of Iceland, 101 Reykjavik, Iceland

<sup>2</sup>Laboratoire d’Océanographie Physique et Spatiale, University of Brest, CNRS, IRD, Ifremer, Plouzané, France

<sup>3</sup>Hafrannsóknastofnun/Marine and Freshwater Research Institute, Hafnarfjörður, Iceland

<sup>4</sup>Woods Hole Oceanographic Institution, Woods Hole, MA, USA

<sup>5</sup>University of Akureyri, Akureyri, Iceland

<sup>6</sup>Unidad oceáno y clima, Instituto de Oceanografía y Cambio Global, IOCAG, Universidad de Las Palmas de Gran Canaria, ULPGC, Unidad Asociada ULPGC-CSIC, Las Palmas de Gran Canaria, Spain

**Correspondence:** Angel Ruiz-Angulo (angel@hi.is)

Received: 5 May 2025 – Discussion started: 21 May 2025

Revised: 4 May 2026 – Accepted: 8 May 2026 – Published: 29 May 2026

**Abstract.** The ocean around Iceland is a key region where major water masses and currents interact, influencing the global ocean circulation. Here, we analyze 29 years (1990–2019) of quarterly hydrographic section data collected around Iceland. The hydrographic properties around Iceland show important spatial variability. Based on temperature, salinity, and stratification structure, we classified the Icelandic waters in three distinct regions: the south, the north, and northeast regions. The warm and salty Atlantic Waters that dominate the south show the deepest winter mixed layers (~ 500 m) while the north and northeast show shallower depths (~ 100 m). Based on the decomposition of total stratification into temperature and salinity contributions, we find that the subsurface stratification is mainly controlled by temperature in the south and by salinity in the northwest, while in the north, the North Icelandic Irminger Current and East Icelandic Current alternate seasonally, shifting the region between temperature-dominated and salinity-dominated stratification. The interannual variability of the mixed layer and of its thermohaline properties is also large around Iceland. Mixed layer waters were generally colder in the 1990’s, then warmed until approximately 2015, and became colder again from 2015 to 2018. In the northeast, a multidecadal mixed layer warming trend emerges from the interannual variability as the Atlantic Water progresses northeastward, which is responsible for transforming locally the upper stratification

from salinity-dominated into temperature-dominated. This is associated with the “Atlantification” of the Arctic. Within the mixed layer south of Iceland, density has continuously decreased since the mid 1990’s. Elsewhere, we observe density-compensated changes in mixed layer temperature and salinity, without clear long trends. This study provides an unprecedented and detailed description of the seasonal to multi-decadal variability of the mixed layer depth and stratification around Iceland, showing links between this regional variability and changing North Atlantic under global warming.

## 1 Introduction

The ocean around Iceland is a key region where major water masses and currents interact, shaping the North Atlantic circulation, and play a crucial role on the Atlantic Meridional Overturning Circulation (AMOC). The Nordic Seas are among the few places on the globe where the formation of deep waters (1000–3000 m depth) occurs during winter deep convection (Petit et al., 2020). The southern end of the Nordic Seas is bounded by the Greenland-Iceland-Scotland Ridge (GISR). The North Atlantic Current (NAC) brings the warm and salty Atlantic Water (AW) northward into the Nordic Seas (Hátún and Chafik, 2018; Østerhus et al., 2019; Hátún et al., 2021). The AW crosses the ridge in three

ways (Fig. 1): (i) between Greenland and Iceland, where the Irminger Current (IC) forms the North Icelandic Irminger Current (NIIC) bringing AW that flows clockwise around Iceland (Jónsson and Briem, 2003; Jónsson and Valdimarsson, 2012); (ii) between Iceland and the Faroe Islands (Mauritzen, 1996); and (iii) through the Faroe Shetland Channel (Hansen and Østerhus, 2000; Hansen et al., 2023), contributing up to 48 % of the total AW transport. The AW undergoes strong cooling and densification in the Nordic Seas and the Arctic Ocean (Mauritzen, 1996; Pérez-Hernández et al., 2019; Athanase et al., 2020; Huang et al., 2023). This modified AW is referred to as Atlantic-origin Overflow Water (AtOW; e.g., Håvik et al., 2017; Casanova-Masjoan et al., 2020) and is one of the two sources of Denmark Strait Overflow Water (DSOW; Semper et al. 2019). AtOW travels southward as a mid-depth water mass in the East Greenland Current (EGC; Håvik et al., 2017), from where, part of it diverts east and merges with the NIIC northeast of Iceland (Casanova-Masjoan et al., 2020).

The transformation of AW into AtOW takes place in different areas of the Nordic Seas: along the Norwegian Current (Håvik et al., 2017), in the Iceland Sea Gyre (Våge et al., 2013), on the eastern side of Greenland, or even – due to its proximity – in the Arctic Basin (Pérez-Hernández et al., 2019). This transformation has different driving mechanisms impacting mixing and convective processes. Wind-stress, sea-ice retreat, and high heat loss due to cold-air outbreaks drive the transformation east of Greenland (Våge et al., 2018). Sea-ice retreat, and heat exchange dominate north of Svalbard (Pérez-Hernández et al., 2019; Athanase et al., 2020), and heat fluxes are the main drivers in the center of Iceland Sea (Våge et al., 2013). Thus, the Nordic Seas region has been previously described as a “mixing pot” (Renfrew et al., 2019), largely responsible for the overall formation of deep overflow water (Lozier et al., 2019). The Nordic Seas are also a large repository of freshwater, primarily originated from glacier melt and river discharge. This water mass increases buoyancy and is carried southward by the East Greenland Current (EGC). Therefore, it is crucial to fully understand the variability of the upper ocean, where mixed layers (ML) develop and transform these water masses.

The Arctic Ocean is warming much faster than the global average, a process known as “Arctic Amplification”, which is also associated with the “Atlantification” of the Arctic (Polyakov et al., 2017; Dai et al., 2019). While the causes are still debated, Arctic Amplification has evident consequences, such as a decrease in seasonal sea-ice extent and a weakening of the cold halocline (Polyakov et al., 2020; Dai et al., 2019). Although these changes are less pronounced in the central Iceland Sea, similar processes have been observed in the central Greenland Sea and the northeastern shelf (Gjelstrup et al., 2022; Strehl et al., 2024), suggesting that Atlantification may also influence the Iceland Sea. Changes in temperature and salinity in the upper ocean modify upper-

ocean stratification, which partially controls the mixed layer depth (MLD).

The depth and structure of the ML is primarily controlled by local buoyancy forcing, i.e., surface heat loss and freshwater fluxes, which modifies the water density (Kohler et al., 2018). For instance, within the Iceland Basin, wintertime buoyancy loss drives deep convection, shaping the thermohaline properties that influence the lower limb of the AMOC and its variability in the subpolar North Atlantic (Petit et al., 2021). The pre-existing stratification of the water column is responsible for controlling the effect of the surface forcing. Strongly stratified upper layers resist mixing, while weak stratification allows deeper penetration of turbulence and convection mixing (Pierce et al., 1986). Over shorter timescales, on the order of days, the MLD can significantly deepen as a result of the strong wind events with significant wind stress and associated large wave heights (Skylvingstad et al., 2023). MLD and stratification are strongly influenced by atmospheric forcing, including variability associated with the North Atlantic Oscillation (NAO), which modulates wind stress, surface heat flux, and freshwater input in the Iceland region (Hurrell, 1995; Dickson et al., 1996)

The Intergovernmental Panel on Climate Change (IPCC), Special Report on the Ocean and Cryosphere in a Changing Climate (IPCC-SROCC 2019), indicates with *high confidence* that roughly 40 % of the global ocean mean upper ocean stratification has increased about 3.3 %–6.1 % since 1960 due to both oceans warming and high-latitude freshening (Tesdal et al., 2018; Yamaguchi and Suga, 2019; Bindoff et al., 2019; Li et al., 2020; Liu et al., 2020; Sallée et al., 2021). Increased stratification is associated with less efficient diapycnal mixing, reducing the exchanges of heat and tracers from the mixed layer into the ocean interior. It has also been observed, with *high confidence*, that the ML is undergoing changes (Bindoff et al., 2019; on Climate Change, IPCC). Particularly, the shallow summertime ML, which is more likely to be affected by global warming, is deepening at a rate of 5–10 m per decade (Sallée et al., 2021). Despite the reported global patterns, it has been also acknowledged that regional changes might differ from the global estimates (Fox-Kemper et al., 2021).

The warming of the ML and the associated increase in stratification have an impact in biogeochemical processes like phytoplankton blooms and carbon or oxygen sequestration, key components for the Earth’s climate (Ólafsson, 2003; Pérez et al., 2021). In the waters surrounding Iceland, the phytoplankton community is closely linked with the water mass properties and hence, an “Atlantification” will replace Polar communities with more Atlantic communities (Cerfonteyn et al., 2023). In the Arctic Ocean, north and northwest of Iceland, the early onset of stratification in spring gives rise to rapid shallowing of the mixed layer and triggers early spring phytoplankton blooms, whereas the weakly stratified water-column in the Atlantic water and the associated deep ML delay the spring bloom south of Iceland

(Zhai et al., 2012). This also has strong consequences in carbon uptake, vertical nutrient supply, and biological processes (Yamaguchi and Suga, 2019). Other indirect impacts of the increased stratification include changes in upwelling, deep-water formation rates, biological production, and remineralization rates (Holt et al., 2016), and deoxygenation (Shepherd et al., 2017).

Thus, the overall goal of this study is to characterize the spatial and temporal variability of the mixed layer and stratification around Iceland, where Atlantic Water inflow, Arctic waters, and local surface fluxes shape upper-ocean properties. Using a 29-year hydrographic time series, we investigate the variability of water-mass properties, mixed-layer depth (MLD), density, and thermohaline structure across seasonal and interannual timescales. We examine correlations with atmospheric circulation patterns such as the North Atlantic Oscillation (NAO) and, to complement the observations, use a 1D PWP model to simulate the mixed-layer response to local forcing, helping to identify the mechanisms driving MLD variability.

## 2 Data and methods

We use Conductivity-Temperature-Depth (CTD) data from the repeated hydrographic observational program of the Icelandic Marine and Freshwater Research Institute between 1990 and 2019. The oceanographic surveys took place quarterly, mainly in February, May, August, and November with little coverage during the intermediate months. Observations are made at standard repeated sections. The profiles are obtained with a Seabird 911plus CTD mounted on a rosette with Niskin bottles. The conductivity data are calibrated with salinity samples taken at the bottom of each station. All sensors underwent regular calibrations by the manufacturer.

In our analyses we considered only the deepest stations in each section (red dots in Fig. 1), including nearby stations within an area defined by  $1^\circ \times 0.5^\circ$  in longitude and latitude (red boxes). The selected stations are located outside of the Icelandic shelf (about 500 m depth). This criterion was chosen to avoid topographic effects, such as across shelf processes on the stratification of the water column and to avoid MLDs limited by shallow bathymetry. Thus, the stations in gray, HB and IH in Fig. 1 were not considered as they fall on the shelf. For the sake of simplicity stations will be named with the acronym of the standard section, first two letters and the station number. The station full name (section and station number) can be found in Table 1.

In this study we analyze the inter-annual variability and linear trends of the ML over a 29-year period as well as the seasonal variability using the seasonal extremes (summer and winter), when there is more data coverage. From the CTD stations we estimated the MLD using the density threshold method with a criterion of  $\sigma_\theta = 0.01 \text{ kg m}^{-3}$  (as, for instance, in Piron et al. (2016) in the Irminger Sea) and

a reference depth of 10 m. We chose this criterion instead of the usual  $0.03 \text{ kg m}^{-3}$  (de Boyer Montégut, 2004) as the latter overestimated the MLD in more than 500 visually inspected profiles (not shown). For comparison and robustness of our chosen method, we also estimated the MLD using other criteria (de Boyer Montégut et al., 2004; Holte et al., 2017). We found the density threshold method appropriate for our region as it proves to be effective even for cases where the variations of salinity and temperature were large. Those variations usually compensate in density making this method more suitable. We have validated our method against previous work by Våge et al. (2018), where a glider data were available, and the results were satisfactory. However, automatic detection methods have limitations, as they may miss stacked mixed layers and other non-canonical representation MLs.

For each profile we computed the Brunt-Väisälä frequency ( $N^2$ ), defined as:

$$\rho N^2 = g \frac{1}{\rho_0} \frac{\partial \sigma_\theta}{\partial z}, \quad (1)$$

where  $g$  is the acceleration due to gravity,  $\rho_0$  is a reference density,  $\sigma_\theta$  is the potential density and  $z$  is depth.  $N^2$  can be decomposed to show the relative contribution of salinity and temperature to the observed stratification as follows:

$$N^2 = N_T^2 + N_s^2 \quad (2)$$

where  $N_T^2$  and  $N_s^2$  are the components representing the stratification set by the temperature and salinity, respectively and are defined as:

$$N_T^2 = g \left( \alpha \frac{\partial T}{\partial z} \right) \quad (3)$$

$$N_s^2 = g \left( \beta \frac{\partial S}{\partial z} \right), \quad (4)$$

where  $\alpha$  is the thermal expansion coefficient and  $\beta$  is the haline contraction coefficient at constant pressure. This decomposition has also been made to classify the oceans by their stratification contribution into  $\alpha$ -ocean,  $\beta$ -ocean, and transition zone, where in  $\alpha$ -oceans stratification is permanently dominated by temperature, in  $\beta$ -oceans by salinity and the transition regions are either intermittently or seasonally dominated by temperature or salinity (Carmack, 2007; Stewart and Haine, 2016). For the water column to be statically stable,  $N^2$  must be positive. However, the contributions may not be positive; when either of its components,  $N_T^2$  or  $N_s^2$  are negative, temperature or salinity respectively has a destabilizing effect on the resulting stratification that must be compensated by the other variable to maintain a stable water column. Small values of  $N^2$  indicate that the water column is weakly stratified, which favors mixing due to winter convection and deeper MLD.

To investigate further the driving mechanism of the MLD, we used the Price-Weller-Pinkel (PWP) model (Pierce et al.,

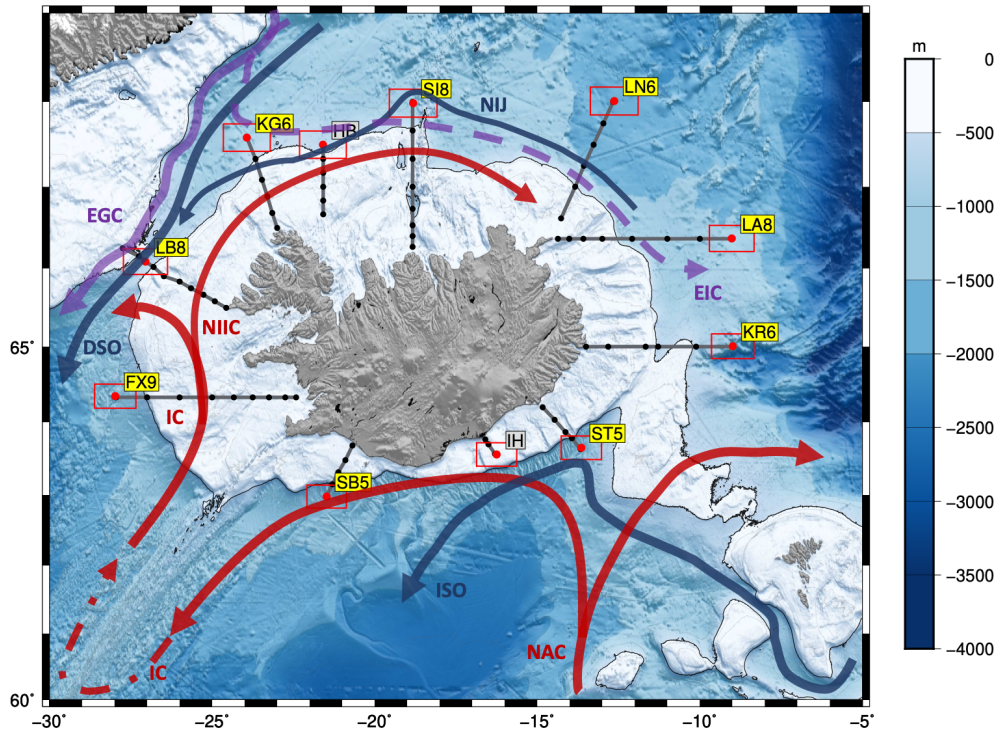


**Figure 1.** Map of the typical hydrographic sections collected by the Marine and Freshwater Research Institute around Iceland; the black dots represent the nominal location of the standard stations from 1990–2019. The red dots are the stations used for this analysis and the red boxes delimit the area within which all data were considered for this study. The grey bathymetric contours are spaced every 100 m for the shallow water until the 500 m depth (thick black line) and then every 500 m. The hydrographic stations shown in the yellow boxes corresponding to the standard sections: Faxaflói (FX9), Látrabjarg (LB8), Kögur (KG6), Hornbanki (HB), Siglunes (SI8), Langanes NE (LN6), Langanes E (LA8), Krossanes (KR6), Stokksnes (ST5), Ingólfshöfði (IH) and Selvogsbanki (SB5). The gray labeled IH and HB were not used in this analysis. The main surface and deep currents are also depicted on the map.

1986). The PWP model was chosen to test the hypothesis that  $\beta$ - and transition oceans do not develop deep mixed layers, which is shown in Fig. 8. The PWP model is a one-dimensional vertical model used to simulate the evolution of the ocean mixed layer in response to atmospheric forcing, including wind stress, heat fluxes, and freshwater fluxes. The model evolves vertical profiles of temperature, salinity, density, and horizontal velocity based on surface forcing and a set of physical stability criteria. The first criterion is convective overturning. If surface cooling increases the density such that the water column becomes gravitationally unstable (i.e., denser water overlies lighter water), the model applies vertical mixing until static stability is restored. The second criterion is based on the Bulk Richardson number, which represents wind-driven mixing. The mixed layer deepens until the Bulk Richardson number ( $Ri_b = (g\Delta\rho h)/(\rho_0(\Delta U)^2)$ ) reaches or exceeds the critical values 0.6. The final criterion is the Gradient Richardson Number  $Ri_g = N^2/(\partial U/\partial z)^2$  which accounts for shear instability. When  $Ri_g < 0.25$ , local vertical mixing is applied. The PWP model is initialized with the ERA-5 12 h dataset of wind stress, heat, and freshwater fluxes (Hersbach et al., 2020) and the summer/winter averaged vertical profiles of temperature and salinity from the ob-

servations presented here (Fig. S1–3). The 1D model allows us to address the relative contributions from diurnal heating/cooling, freshwater fluxes, and wind mixing.

In addition, we broaden the impact of our findings by using the hydrographic database published in Brakstad (2023) that includes, in addition to the dataset from the Marine and Freshwater Research Institute of Iceland, other multiplatform observations like Argo floats or cruise data between 1950 and 2019. For this objective, a larger oceanic region is used and classified into  $\alpha$ -ocean and  $\beta$ -ocean using the spice frequency,  $K^2$ , (Carmack, 2007; Strehl et al., 2024), defined as:

$$K^2 = N_T^2 - N_s^2. \quad (5)$$

$K^2$  is positive in  $\alpha$ -oceans and negative for  $\beta$ -oceans.

### 3 Results

#### 3.1 Hydrographic properties around Iceland

The hydrographic properties (potential temperature-salinity diagrams) around Iceland show important spatial, seasonal, and interannual variability (Fig. 2); the  $T/S$  properties differ

widely between the three representative stations: FX9, SI8 and LN6 for the west, north and northeast of Iceland. FX9, in the southwest of Iceland, is completely dominated by Atlantic Water (AW; Fig. 2a and b). At SI8, in the north, the dominating water masses in winter are of polar origin, i.e., warm Polar Surface Water (PSWw) in the upper layers, and Atlantic Overflow Water (AtOW) and Arctic Overflow Water (ArOW) in the intermediate/bottom waters (Fig. 2c and d). The SI8 station also presents the largest variance of its thermohaline characteristics. It is noteworthy that using fixed definitions of water masses may lead to biased estimates, as these water masses have been steadily warming over the past two decades. LN6, in the northeast, contains the coldest and densest waters on average (Fig. 2c and f).

The three stations have a clear seasonality. Overall, due to seasonal warming of the upper layers, the summer profiles span a wider temperature range (Fig. 2b, d, f) than in winter (Fig. 2a, c, e). FX9 is notably warmer and saltier than the other stations, especially in summer (Fig. 2a), when the minimum temperature in FX9 (nearly 4 °C) is as high as the maximum temperature in SI8 and 2° higher than in LN6 (Fig. 2a, b, c). At SI8 a large change in density between seasons is observed mainly driven by the contribution of AW, explained by offshore migration of the NIIC and the stronger inflow of AW during the summer (Fig. 2c and f) (Jónsson and Valdimarsson, 2012). While the widest seasonal amplitude in salinity is observed at SI8, the largest seasonal amplitude in temperature is observed at LN6.

FX9 does not show a clear interannual pattern in summer, but in winter the 2000's are strikingly saltier than the other years. In contrast, at SI8 and LN6 fresher and colder waters are observed in the 1990's, they progressively warm and become saltier over time, and they reach their maximum temperature and salinity by 2015–2018. This decadal pattern is more evident in winter, but it is observed in both seasons.

### 3.2 Seasonality of Stratification and Mixed Layer Depth (MLD)

The spatial and temporal variability of the stratification around Iceland is remarkably large (Figs. 3 and 4), and the relative contribution of temperature and salinity shows a strong seasonal cycle. In summer, the MLD is relatively shallow, oscillating around 50 m with a small standard deviation (Fig. 3). In contrast, in winter the ML reaches depths greater than 400 m in FX9, ST5 and SB5 with large standard deviations spanning a 100 m range (Fig. 4). The deepest average MLD is found in FX9 while the shallowest are KG6, SI8, LA8 and KR6.

In summer (Fig. 3), the upper-ocean stratification around Iceland (Fig. 3) is generally dominated by temperature, except for the three northwestern stations (namely LB8, KG6, SI8). LB8 exhibit the largest variability in both  $N_T^2$  and  $N_S^2$ , but is mainly dominated by salinity in the upper 200 m and by temperature below that depth. This transition station is

located at the sill of Denmark Strait, a convergence zone for several currents (see Table 1 and Fig. 1) carrying water masses with contrasting  $T$ - $S$  properties within the ML and the thermocline (Jónsson, 1999; Logemann et al., 2013; Casanova-Masjoan et al., 2020). In KG6, the fresh inflow from the EGC compensates for the cold temperature, and salinity largely dominates stratification. For SI8, we observe a mixed regime with almost equal contributions from both salinity and temperature to the total stratification, which suggests that this is also an area of transitional regime. For the stations: LN6, LA8 and KR6, despite the fact that stratification is mainly dominated by temperature, exhibit a small subsurface contribution of salinity just below the ML, likely due to the presence of fresh PSWw. The southern stations ST5 and SB5, have a minimal contribution to stratification from salinity, which may be associated with the numerous river discharges and the proximity to the continental shelf. The river discharge is the largest near SB5, likely explaining the summer subsurface contribution to salinity (Whitney, 2025).

The hydrographic conditions are very different for winter; the stratification is one order of magnitude lower, i.e., comparing Figs. 3 and 4. Also, the water temperature is much colder due to winter heat loss. Under these conditions, the relative contribution of salinity to the total stratification stands out around Iceland except at the southern stations (FX9, SB5, ST5), where the weakest winter stratification is observed. This southern region shows the deepest MLD, between 350 and 700 m in the stations FX9, SB5 and ST5, while for the northern stations (KG6, SI8, LN6, LA8, and KR6) the mean winter MLD is about 100 m. Similar to summer, station LB8, also shows high variability in winter stratification, associated with the confluence of currents at the Denmark Strait.

The role of temperature or salinity in setting the stratification ( $\alpha$ - and  $\beta$ -ocean, see e.g., Carmack, 2007) is linked to the hydrographic characteristics (temperature and salinity) of the dominant water masses within each region. Based on this, we can classify the waters around Iceland. The southern side is an  $\alpha$ -ocean as it receives the influence of warm and relatively salty AW. Hence, the stratification is mainly temperature driven in both seasons (see FX9, ST5 and SB5 in Figs. 3 and 4) and MLD gets deeper than 400 m in winter. The northwest of Iceland (LB8, KG6) is under the influence of the EGC throughout the year bringing fresh PSW and PSWw into the area. Therefore, this area with winter MLDs of 100–150 m can be considered a  $\beta$ -ocean, with heat fluxes equivalent to the southern region but with stronger and salinity dominated stratification blocking the potential for deep convection, i.e., this region does not have a mechanism to lose surface buoyancy seasonally in the salinity component. In contrast, the northeastern Icelandic area (SI8, LN6, LA8 and KR6) shifts from  $\beta$  in winter to a mixed  $\alpha/\beta$  in summer. This is likely due to an offshore migration of the NIIC increasing the inflow of AW (Jónsson and Valdimarsson, 2012;

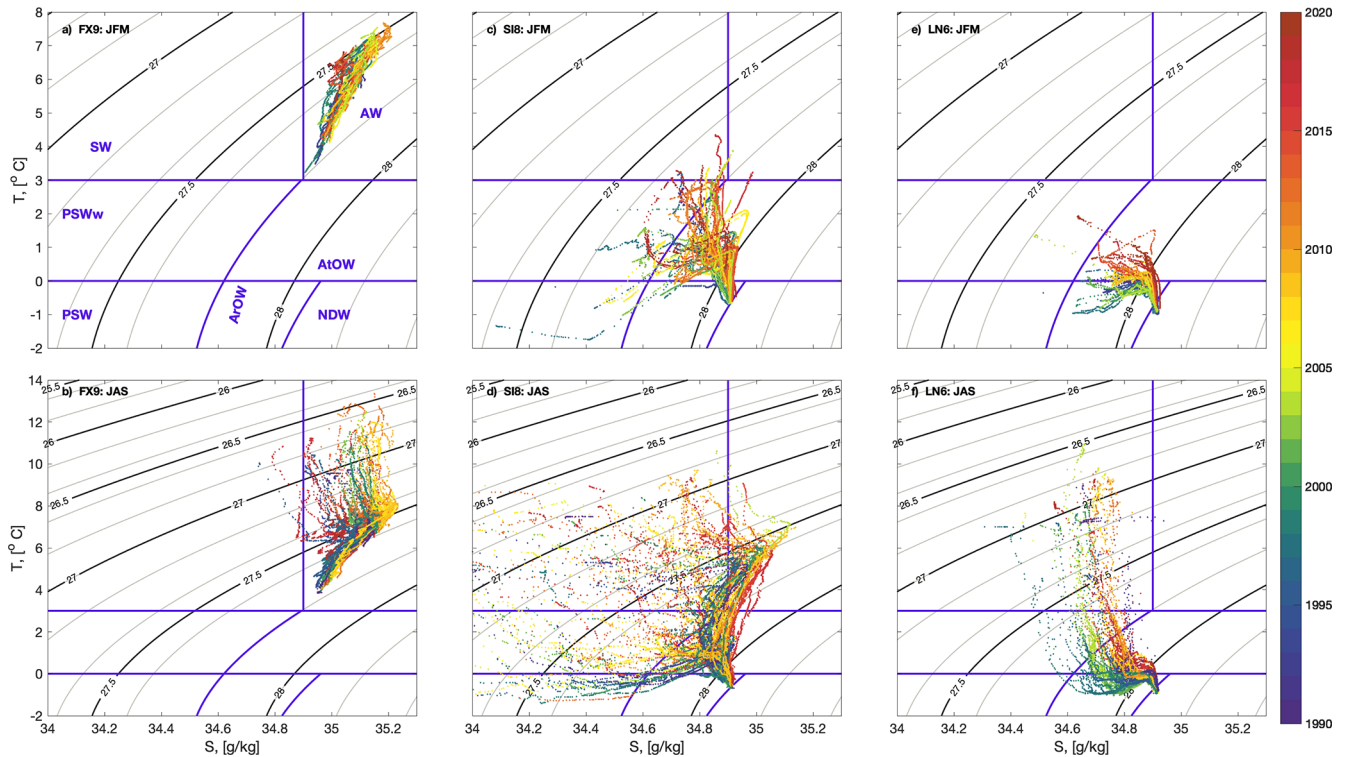


**Figure 2.** (Top row) Winter (JFM) and (bottom row) summer (JAS)  $T$ - $S$  diagrams for three selected stations (a, b) FX9, (c, d) SI8 and (e, f) LN6, considered as representative for the south, north and northeast regions shown in Fig. 1. The  $T$ - $S$  individual profiles are color-coded by year. The main water masses as defined in Table 2, are labeled in panel (a).

Casanova-Masjoan et al., 2020, their Fig. 11). For instance, in winter, SI8 has a PSW signature at the thermocline with salinity driving the stratification and a MLD of about 90 m ( $\beta$ -ocean), and in summer, the NIIC brings warm AW to the upper layers of SI8 making the stratification similarly driven by temperature and salinity. Overall, the north of Iceland exhibits the strongest summer stratification of the study area which results in very shallow MLDs.

### 3.3 Interannual to decadal variability of the mixed layer properties

To investigate the interannual to decadal ML variability we focused on three reference stations, considered representative of the  $\alpha$ -ocean (FX9, west), transition (SI8, north) and  $\beta$ -ocean (LB8, northwest) regimes around Iceland. FX9 dominated by relatively warm and salty AW, SI8 as a transition area, and LB8 dominated by cold and fresh PSW. The three stations show strong interannual variability.

In FX9, to the west of Iceland, there is a correlation ( $R = 0.69$   $p$ -value  $< 0.01$ ) between mixed layer temperature (MLT) and salinity (MLS) anomalies. Between 1990 and 1998 the mixed layer was the deepest, the coldest, and the second freshest period, as shown in Fig. 5a and d (positive MLD anomalies correspond to deeper ML and negative ones correspond to shallower ML). Around the period 2000–

2014, there is an increase in MLT and MLS as the ML becomes moderately shallower. The winter MLD is the shallowest, saltiest, and warmest in 2010 (Fig. 5a and d), when the temperature contribution seems to control this minimum. From 2015 to 2018 the ML returns to the cold and fresh conditions of the 1990's but the MLD is near its long-term average. The observed variability of the ML and its temperature in FX9 exhibits correlation ( $R$ ) with the North Atlantic Oscillation (NAO); for MLD, the best correlation was  $R = 0.53$ ,  $p$ -value  $< 0.01$  at lag zero; for MLS  $R = -0.52$ ,  $p$ -value  $< 0.01$  at lag  $-2$  years (NAO leading), and for MLT  $R = -0.49$ ,  $p$ -value  $< 0.01$  at lag  $-1$  year (NAO leading (Fig. 5g, h). However, in our assessment, the 2-year lag lacks a plausible physical explanation; therefore, we do not consider it a reliable correlation. More qualitatively, positive NAO at the beginning and the end of the time series, corresponds with deeper, colder, and fresher MLs, while negative NAO between 2000 and 2015 roughly corresponds with shallower, warmer, and saltier MLs. As shown in Fig. 2, FX9 contains only AW (Fig. 2a, d) likely advected from the south to the area by the Gulf Stream and later the Irminger Current. Similar conditions have been observed in the Irminger Sea over the same period, and they have been related to the NAO phase and its impact on the Subpolar gyre (Feucher et al., 2022). This suggests that the FX region is largely influenced

**Table 1.** Characteristics for the representative stations for each typical surveyed section. The representative ocean currents at each section are also shown: North Icelandic Irminger Current (NIIC), Irminger Current (IC), East Greenland Current (EGC), North Icelandic Jet (NIJ), East Icelandic Current (EIC), and North Atlantic Current. (NAC). The corresponding stratification regimes are listed for summer and winter for each station.

| Station            | Depth (m) | Lon     | Lat    | Oceanic region                 | Significant currents | Stratification regime                              |
|--------------------|-----------|---------|--------|--------------------------------|----------------------|--|
| Faxaflói (FX9)     | 1010      | −27.98  | 64.35  | Subpolar North Atlantic        | IC                   | Alpha-ocean (summer)<br>Weakly stratified (winter) |
| Látrabjarg (LB8)   | 658       | −27.050 | 66.083 | Denmark Strait                 | NIIC, EGC, DSO       | Beta-ocean (all year round)                        |
| Kögur (KG6)        | 980       | −23.933 | 67.583 | Western Iceland Sea            | EGC, DSO             | Beta-ocean (all year round)                        |
| Siglunes (SI8)     | 1023      | −18.83  | 68.00  | Kolbeinsey Ridge               | NIIC, EGC, EIC, NIJ  | Transition (summer)<br>Beta-ocean (winter)         |
| Langanes NE (LN6)  | 1850      | −12.66  | 68.00  | Iceland Sea                    | EIC                  | Alpha-ocean (summer)<br>Beta-ocean (winter)        |
| Langanes E (LA8)   | 1251      | −9.00   | 66.37  | Iceland Sea                    | EIC                  | Alpha-ocean (summer)<br>Transition (winter)        |
| Krossanes (KR6)    | 1419      | −9.00   | 65.00  | Iceland Sea/<br>North Atlantic | EIC, NAC             | Alpha-ocean (summer)<br>Transition (winter)        |
| Stokksnes (ST5)    | 1153      | −13.66  | 63.66  | North Atlantic                 | NAC                  | Alpha-ocean (summer)<br>Weakly stratified (winter) |
| Selvogsbanki (SB5) | 1006      | −21.48  | 62.98  | North Atlantic                 | IC                   | Alpha-ocean (summer)<br>Weakly stratified (winter) |

**Table 2.** Main water masses definitions for the region of study (Rudels et al., 2005; Våge et al., 2011).

| Water mass                                   | Potential Temperature ( $\theta$ )              | Salinity      | Potential density ( $\sigma_0$ , $\text{kg m}^{-3}$ ) |
|--|---|---------------|---|
| Surface Water (SW)                           | $> 3^\circ\text{C}$                             | –             | $\sigma_0 < 27.70$                                    |
| Warm Polar Surface Water (PSW <sub>w</sub> ) | $0^\circ\text{C} \leq \theta < 3^\circ\text{C}$ | –             | $\sigma_0 < 27$                                       |
| Polar Surface Water (PSW)                    | $< 0^\circ\text{C}$ ,                           | –             | $\sigma_0 < 27.70$                                    |
| Atlantic Water (AW)                          | $> 3^\circ\text{C}$                             | $> 34.9$      | –   |
| Atlantic-origin Overflow Water (AtOW)        | $0^\circ\text{C} \leq \theta < 3^\circ\text{C}$ | –             | $\sigma_0 \geq 27.8$ , $\sigma_{0.5} < 30.44$         |
| Polar intermediate Water (PIW)               | $0^\circ\text{C}$                               | $\leq 34.676$ | $\sigma_0 > 27.70$                                    |
| Arctic-origin Overflow Water (ArOW)          | $< 0^\circ\text{C}$                             | –             | $\sigma_0 > 27.8$ , $\sigma_{0.5} < 30.44$            |
| Nordic Seas Deep Water (NDW)                 | $< 0^\circ\text{C}$                             | –             | $\sigma_{0.5} \geq 30.44$                             |

by the Atlantic climate and therefore it is partly impacted by the NAO (Bersch, 2002).

At SI8, in the north of Iceland (Fig. 5b, e, h), the negative winter MLD anomalies are on the order of those at FX9 and also exhibit strong interannual variability without an identifiable pattern. Strong positive MLD anomalies are observed in particular years (e.g., 2000, 2007, and 2016), but they do not seem correlated with the MLT/MLS or with the NAO variability. Interestingly, the MLT and MLS co-vary during the period 1990–2005, when the mixed layer is colder and fresher, but this correlation weakens from 2005–2018, when

the positive MLT anomalies increase while the MLS anomalies, although positive, do not vary significantly.

In LB8 (northwest), the winter MLD has the largest variability as the station is located in the vicinity of the front between NIIC and the EGC, which shapes the Polar and Atlantic conditions. Despite this large variability, a co-variance between MLT and MLS anomalies seems to be correlated with the position of the front. Fresher and colder MLs are associated with EGC influence and warmer/saltier MLs with the presence of NIIC (Fig. 5c, f, l). Generally, shallower MLs are also fresher and colder, which agrees with a salinity-dominated stratification in the upper layer (Fig. 4b). Three

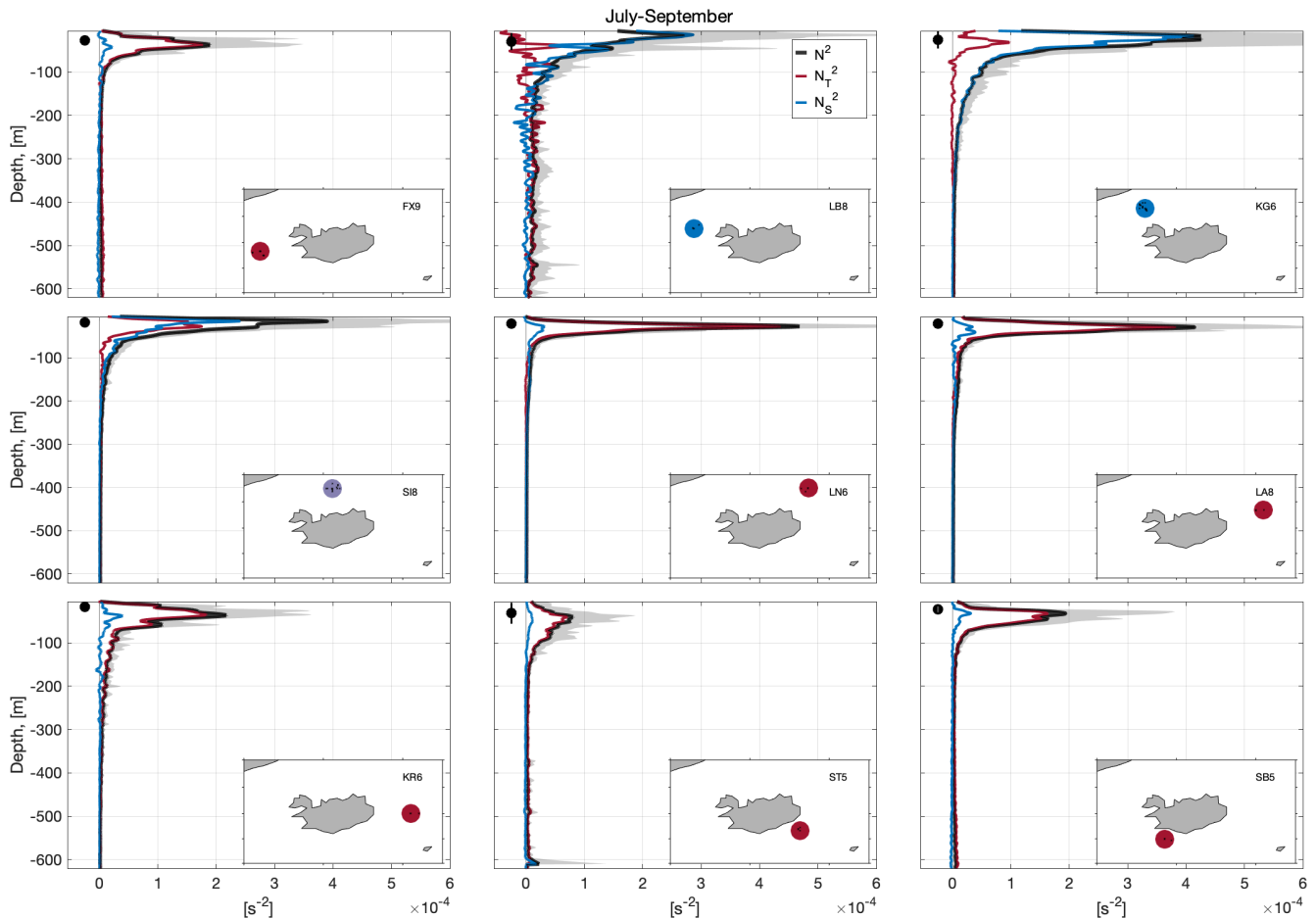


**Figure 3.** Summer (JAS) average density stratification ( $N^2$ ) profiles for the selected stations; the average total stratification (black) is decomposed into temperature (red) and salinity (blue) contributions, while the gray shaded band represents all the stratification profiles. The black solid dot (left of the profiles) represents the average MLD with the error bar showing the standard deviation as an indicator of the temporal variability. The maps in the lower corner show the location of the station within a circle color coded by the dominating regime according to the contribution to stratification: red for temperature, blue for salinity, and purple for a mixed regime.

particular years present relatively deep, cold, and salty MLs: 1996, 2006 and 2014. The observed interannual variability in the ML and its properties, while large, does not seem to be correlated with the NAO, except during the last decade, when the high state of the NAO is consistent with the positive MLT and MLS, suggesting a larger presence of the NIIC at this station.

To delve into the interannual to decadal variability of the MLT around Iceland, we analyzed its anomalies (relative to the long record) in all nine stations and computed their linear trends (Fig. 6). The temperature anomalies show significant interannual variability and spatial differences around Iceland. For instance, positive anomalies were observed in 2003 in most of the stations in both seasons, with particularly large temperature anomalies east of Iceland. Strong warm anomalies are also observed in 2017, mostly in summer at all stations except FX9 and SB5, located south of Iceland (Fig. 6; left panel). Although the 29-year period might be too short

for identifying linear anthropogenically-driven trends, linear trends are significant in some of the stations, (where the  $p$ -value is indicated). The linear trends show a general warming of the mixed layer that is more evident in winter, mainly in the stations of the northeast (LN6, LA8). In the south (ST5, SB5 and FX9), even if the trend is significant from 2000–2015, there is an interannual variability that induces colder mixed layer conditions from 2015 to 2018. This tendency of returning to the conditions observed in the early 1990's may be associated with the NAO (Feucher et al., 2022) as shown in Fig. 5. The observed general warming of the ML around Iceland is consistent with the progressive warming of the NIIC (Casanova-Masjoan et al., 2020).

Similarly to Fig. 6, in Fig. 7 we compute the winter (JFM) density within the ML, which exhibits a statistically significant decrease for the stations in the south of Iceland (FX9, SB5, and ST5). The rest of the stations around Iceland do not show any significant changes. Remarkably, LN6, LA8, and

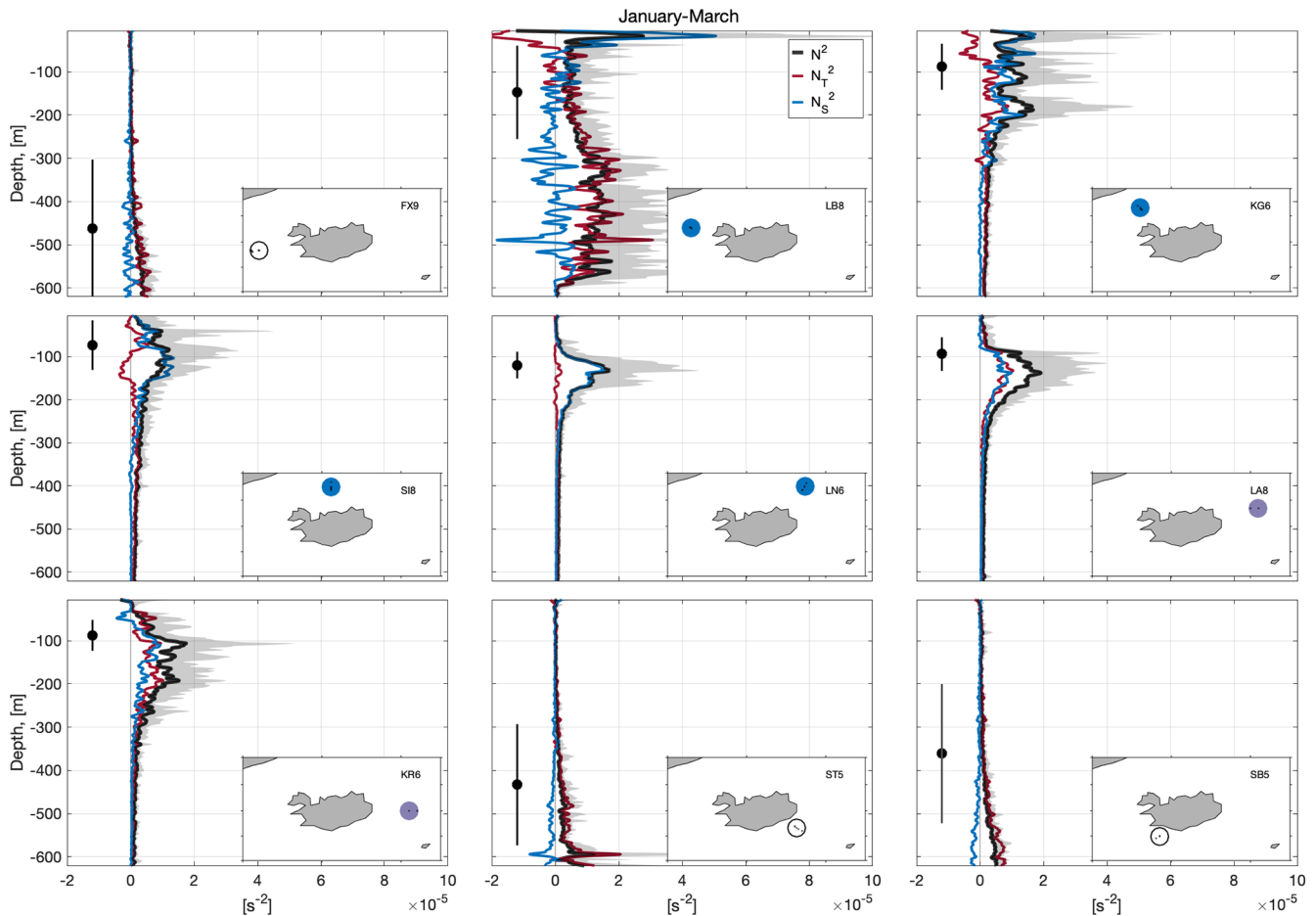


**Figure 4.** Same as Fig. 3 but for winter (JFM). The white color circles shown in the maps of stations ST5, SB5, and FX9 indicate very weak winter stratification with no significant contribution of salinity or temperature.

SI8 show no change in density even though they experience a significant increase in temperature.

#### 4 MLD driving mechanisms from a 1D model

The stratification around Iceland in summer is roughly an order of magnitude higher than in winter, largely due to positive buoyancy forcing, resulting in shallower and more variable MLDs. Therefore, we study the atmospheric effect on these  $\alpha$ - and  $\beta$ -ocean regions by implementing the Price et al. (1986) one-dimensional model. The model is forced starting in the fall before the deep MLD develops. The model results of the MLDs shown in Fig. 8 are within the range of the observed average  $\pm$  standard deviations (thick black dots and lines in Fig. 8). For most stations a spring shoaling of the MLD is driven by reduced heat fluxes, while the MLD remains relatively deep due to the wind-stress.

In the model, the stations embedded within the  $\alpha$ -ocean with AW (Fig. 8: FX9, SB5 and ST5) present the largest MLDs exceeding 300 m depth, which is consistent with the

observations. In this  $\alpha$ -ocean region, the development of a deep ML is driven mainly by heat. However, within these stations, the wind-stress steadily contributes to the development of the ML. During the summer, shoaling of the mixed layer is likely influenced by the changes of both heat and freshwater fluxes, with their effects on the MLD partially offset by wind stress (Fig. 8: FX9, SB5 and ST5).

The station LB8, despite being in Denmark Strait and presenting a large contribution of PSWw and PSW in the upper layers (driving a  $\beta$ -ocean stratification), shows that the development of MLDs can be influenced by both, heat flux and/or wind stress (Fig. 8: LB8). However, the contribution of wind-stress and freshwater cannot lead to MLDs deeper than 100 m (Fig. S4: LB8). Beneath the PSW and PSWw at LB8 we find AtOW. Hence as the wind-stress develops, the MLD evolution erodes the PSWw strata reaching the AtOW layer, allowing reduced heat fluxes to contribute to the MLD development. This erosion is not visible on the stations embedded within the EIC.

Wind stress becomes the leading forcing mechanism northeast of LB8 at stations KG6, and SI8, coinciding with

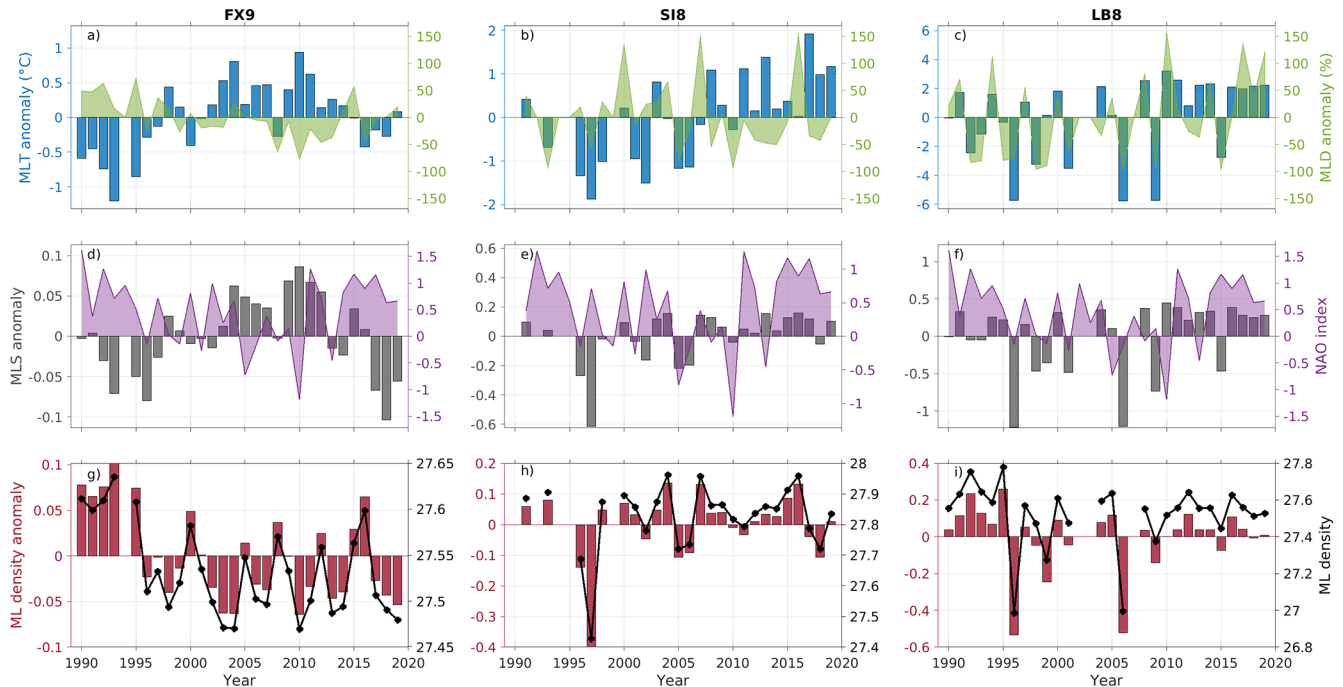


**Figure 5.** Interannual winter (JFM) variability from 1990 to 2019 in three stations representative of different regions around Iceland: (a, b, c) MLD anomaly (in percentage of its mean winter value over the whole record, green shading) and mixed layer temperature (MLT, blue bars). (d, e, f) Mixed layer salinity (MLS, grey bars) and winter average NAO index for comparison (purple shading). (g, h, i) Mixed layer density anomaly (MLrho, red bars) and Mixed layer density ( $\text{kg m}^{-3}$ ), black dots. The represented stations are (a, d) FX9, in the southwest, (b, e) SI8, in the north, and (c, f) LB8 in the northwest. Positive anomalies in MLD, MLS, MLT, and MLrho correspond to deeper, saltier, warmer, and denser waters, respectively. The summary of the correlations is presented in Table 3.

**Table 3.** Summary of the Pearson correlation coefficients between the different variables shown in Fig. 5. Non-significant correlations are omitted. The displayed correlations are significant at 95 % confidence ( $p < 0.05$ ), and those significant at 99 % ( $p < 0.01$ ) are shown in bold.

|         | FX9                     |                            | SI8                    |                           | LB8                    |                           |
|---------|-------------------------|----------------------------|------------------------|---------------------------|------------------------|---------------------------|
|         | Correlation             | <i>p</i> -value            | Correlation            | <i>p</i> -value           | Correlation            | <i>p</i> -value           |
| MLT-MLS | <b><i>R</i> = 0.69</b>  | <b><i>p</i> &lt; 0.01</b>  | <b><i>R</i> = 0.74</b> | <b><i>p</i> &lt; 0.01</b> | <b><i>R</i> = 0.95</b> | <b><i>p</i> &lt; 0.01</b> |
| MLT-MLD | –                       | –                          | –                      | –                         | <b><i>R</i> = 0.76</b> | <b><i>p</i> &lt; 0.01</b> |
| MLS-MLD | –                       | –                          | –                      | –                         | <b><i>R</i> = 0.68</b> | <b><i>p</i> &lt; 0.01</b> |
| NAO-MLD | <b><i>R</i> = 0.53</b>  | <b><i>p</i> &lt; 0.01</b>  | –                      | –                         | –                      | –                         |
| NAO-MLT | <b><i>R</i> = -0.41</b> | <b><i>p</i> &lt; 0.003</b> | –                      | –                         | –                      | –                         |
| NAO-MLS | –                       | –                          | –                      | –                         | –                      | –                         |

the shift from  $\alpha$ - to  $\beta$ -ocean stratification (Fig. 8). This region has a lower convective potential than regions with pure AW and therefore does not produce large MLDs (Figs. 4 and 8). The MLD there results from roughly equal contributions of convection and wind-driven mixing. At these stations, the best performance of the PWP model is obtained when both heat flux and wind-stress are included (Fig. S4). Notably, the summer MLD remains shallow and is roughly the same order of magnitude across all stations around Iceland (Figs. 8 and S4).

## 5 Stratification around Iceland

To complement the understanding of the stratification of the Arctic and Subarctic waters around Iceland, their connection with water masses, currents, and their variability, we used the spice frequency averaged in the first 200 m, estimated following the methods described in Strehl et al. (2024) implementing Eq. (5). For this analysis we used the hydrographic dataset in Brakstad et al. (2023). The spiciness distributions shown in Fig. 9 reveal that temperature dominates on the southern side of Iceland, marked by an  $\alpha$ -ocean regime, while salinity dominates the northern side, associated with

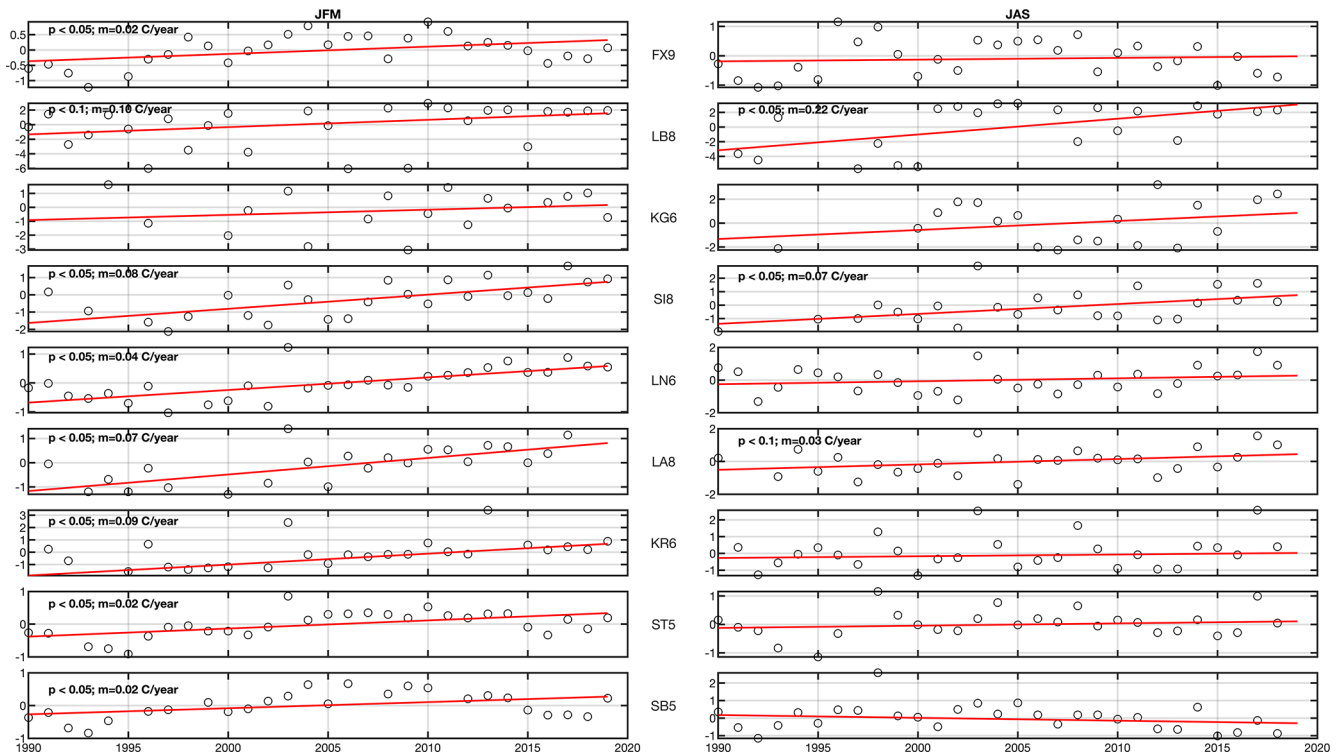


**Figure 6.** Mixed Layer Temperature (MLT) anomaly time series (left) winter (JFM) and (right) summer (JAS) for the 9 stations shown in Figs. 3, 4. The anomalies show the  $p$ -values and the linear trends.

$\beta$ -ocean. These areas largely correspond with the distribution of AW versus PSW/PSWw (See Fig. 2 for  $T$ - $S$  definitions).

The seasonal distribution of spice frequency north of Iceland agrees with the seasonal behavior of the NIIC described in Casanova-Masjoan et al. (2020) where the NIIC surface extension in winter and spring remains constrained to the northwestern side of Iceland due to the cold southeast surface imprint of the EIC. In summer, the NIIC expands northeastward, reaching all the way to the eastern side of Iceland and the northernmost station at the SI transect and constraining the polar water between the northern end of the Kolbeinsey Ridge and the Greenland shelf. In fall, the NIIC northern extension narrows but is still able to surround Iceland. It is noteworthy that a clear increase in coverage of the  $\alpha$ -ocean, mainly in summer, is observed by comparing the 1980–200 average and the 2000–2010 average.

## 6 Discussion and conclusions

In this study, we discussed the seasonal and interannual variability of the mixed layer characteristics and the stratification regimes around Iceland by using a long time series of CTD data. Based on our results, we propose the regionalization of the waters around Iceland into three dynamical regions  $\alpha$ -ocean,  $\beta$ -ocean, and transition-ocean.

The southwestern region is dominated by AW both in winter and summer. Within this region, the winter MLD is the deepest and most variable of the whole study area, with ML's occupied by AW over the whole sampling period. This region is influenced by the dynamics of the Irminger Sea and the Subpolar gyre and has favorable conditions ( $\alpha$ -ocean) for winter deep convection driven by heat fluxes to develop deep mixed layers, which agrees with previous studies (Carmack, 2007; Våge et al., 2008; Piron et al., 2016; Stewart and Haine, 2016; Petit et al., 2020). In the southern region, the ML salinity anomaly was negative over the last 5 years, which is consistent with previous numerical models and Argo observations showing a freshening trend of the North Atlantic (Tesdaal et al., 2018; Holliday et al., 2020; Liu et al., 2020). However, since the south of Iceland is an  $\alpha$ -ocean, these recent changes have not yet reached or affected the MLD.

The northwestern region, which includes the Denmark Strait, is a medley of all the water masses described in this study. In this region there is a confluence of Greenland shelf and slope waters and Iceland Sea origin waters (Harden et al., 2016; Foukal et al., 2020). This includes the NIIC generating an important variability in the water properties due to complex interactions of the regional currents (Lin et al., 2020; Mastropole et al., 2017). The MLD variability over time at the KG6 and LB8 stations is moderate ( $< 100$  m), except for the years 2000, 2007 and 2016 when the ML was

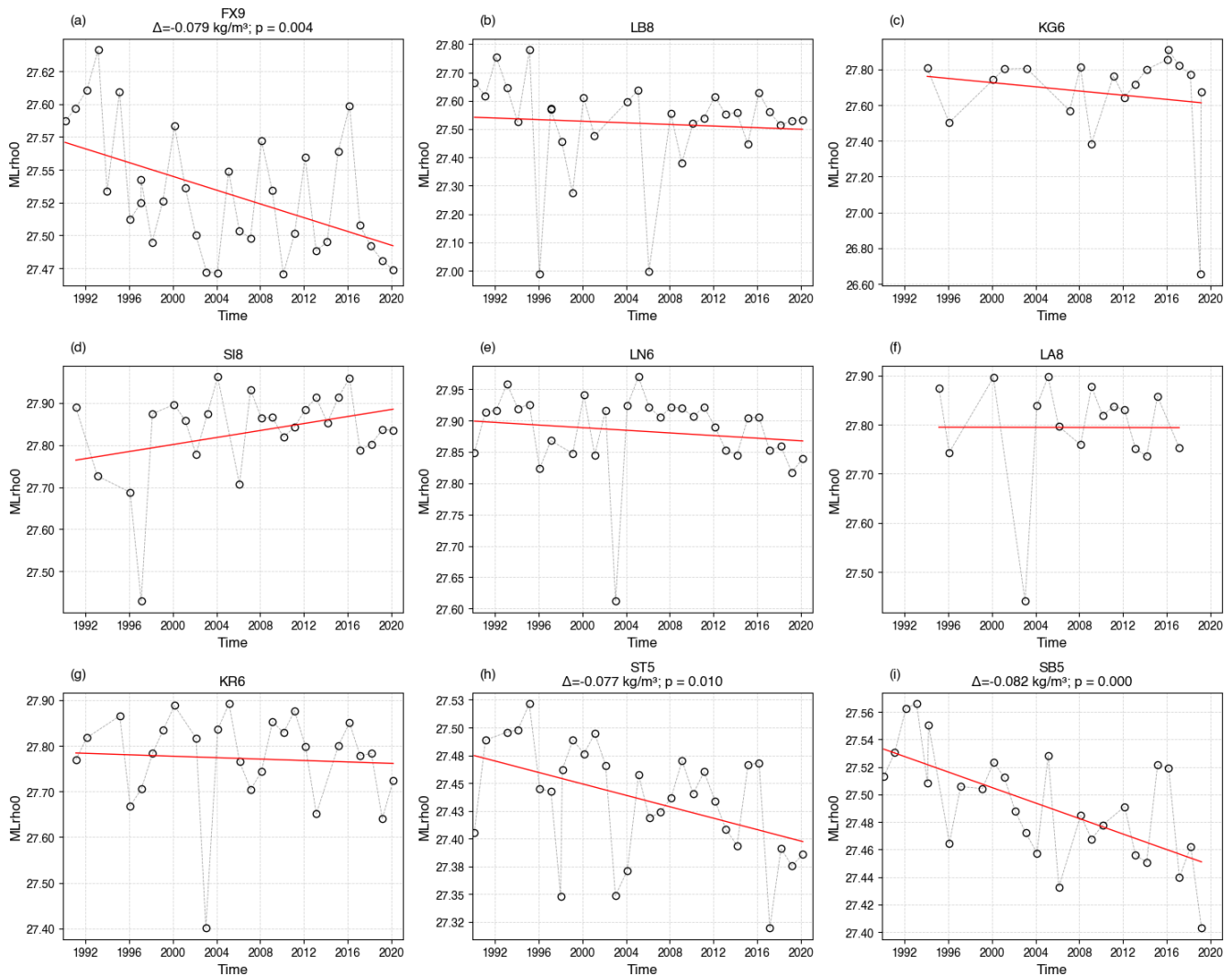


**Figure 7.** Mixed layer density (MLrho) time series for the 9 representative stations only for winter (JFM). Stations FX9, ST5, and SB5 exhibit a statistically significant negative trend, with a total accumulated value of  $\Delta \sim -0.08 \text{ kg m}^{-3}$  over the 29 years of observations.

anomalously deep. In this region, the stratification is notably year-round dominated by salinity ( $\beta$ -ocean), which is explained by the strong Polar influence of cold and fresh waters transported by the EGC. A broader look into the northwestern side of the basin reveals that this area can be divided at the center of the Denmark Strait into an  $\alpha$ -ocean near the Icelandic shelf where the NIIC flows and a  $\beta$ -ocean as we progress towards Greenland (where the LB8 and KG6 stations are located). Near the Icelandic shelf, MLDs are driven mainly by wind-stress, with a secondary contribution of heat fluxes. The  $T$ - $S$  properties as well as the MLT anomalies in the northwest region near the Icelandic shelf show that the NIIC waters there are getting warmer and saltier. This agrees with previous studies showing the transformation of the NIIC also accompanied by an increase in its transport with time (Casanova-Masjoan et al., 2020). Even if the  $\alpha$ -ocean area is warming, it is not expanding northwestward. This suggests

that the EGC may act as a barrier, bringing PSW into the region and maintaining the  $\beta$ -ocean state on the northwesternmost side of the strait. This  $\beta$ -ocean, where the MLD is shallow all year round has dynamical implications as the strong shallow stratification inhibits baroclinic instability and eddy generation (de Marez et al., 2025).

Northeast of Iceland, the ML exhibits intrusions of SW in the winter, while AW is present during the summer. In this region, the stratification changes from  $\beta$ - to  $\alpha$ -ocean seasonally. The Kolbeinsey Ridge acts as a barrier where we find the eastward penetration of the EIC bringing fresh waters (PSWw) from the East Greenland Current (Macranders et al., 2014; Casanova-Masjoan et al., 2020). In summer, the NIIC expands northeastward, bringing AW into the area and changing the stratification regime to  $\alpha$ . Hence, the mixed layer waters show important seasonal variability. They range from maximum temperature below 2 °C in winter to over

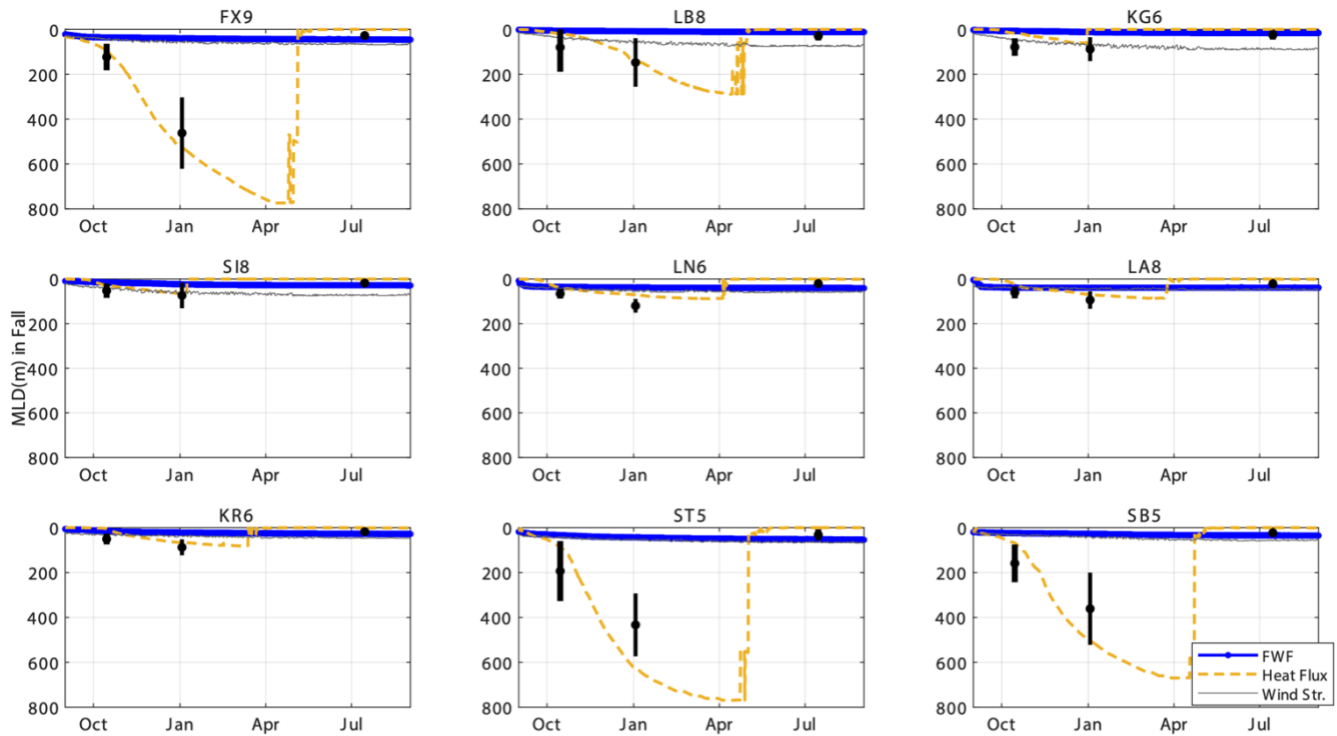


**Figure 8.** MLD driving mechanism decomposition estimated from the PWP 1-D model (Price et al., 1986) for each of the studied stations. Different MLD evolutions are shown for outputs forced with freshwater fluxes (blue), heat fluxes (red), and wind-stress (grey). Black dots represent the mean fall, winter, and summer MLDs with their corresponding standard deviations (black lines).

10 °C in summer. This is also the only region where a significant warming decadal trend emerges over the interannual variability and progressively results in a stronger  $\alpha$ -ocean. This agrees with the AW warming observed in Casanova-Masjoan et al. (2020) and with the northward progression of AW named as “Atlantification” described by Polyakov et al. (2017). This shift to  $\alpha$ -ocean or “Atlantification” may lead to deeper ML’s (Moore et al., 2015; Våge et al., 2022), and the associated deeper convection may increase the potential of this area to contribute to the dense flow carried by the NIJ (Semper et al., 2019).

The regionalization proposed in this work, based on hydrographic properties, matches the recently proposed distribution of primary production around Iceland (Richardson and Bendtsen, 2021; Cerfonteyn et al., 2023), supporting the importance of MLD properties for the primary production (Ólafsson, 2003). The induced alterations on primary production can lead to ecosystem changes. For example, Iceland has witnessed a rapid increase in the population of mackerel, a relatively warm-water fish, since 2006 (Astthorsson et al., 2012; Valdimarsson et al., 2012; Campana et al., 2020) starting from the southeast towards the north, and recently they have been reported almost all around the country. This migration is consistent with the increase in surface temperatures, i.e., northward shift of warmer isotherms over the Iceland Faroe Ridge (de Marez et al., 2025) and the increase of

temperatures within the ML in the same regions over the last decade, which may establish new pathways for entire ecosystems.

The long time series investigated here revealed important interannual oscillations of the ML properties. Five main features are to be highlighted: (i) We do not observe any linear trend in the MLD, which is rather subject to strong interannual variability. (ii) Except for the southern stations, influenced by the subpolar gyre, the interannual variability was not correlated with the NAO. For example, FX9 shows a significant negative of MLT with the NAO ( $R = -0.41$  and  $p$ -value  $< 0.03$ ). (iii) The southern stations, FX9, SB5, and ST5, within the  $\alpha$ -ocean region, show a clear decrease in ML density, with statistically significant values and experience a total decrease during the 29-year period of  $-0.08 \text{ kg m}^{-3}$ . (iv) The linear fit indicates significant (at 95 %) warming trends in the MLT of most of the stations in winter, with the maximum trend of  $0.08 \text{ °C yr}^{-1}$  at S18 resulting in approximately 2.2 °C. This agrees with previous studies (Sarfanov, 2009) showing that the northern part of the North Atlantic (south of Iceland) is strongly dominated by atmospheric interannual to decadal variability, particularly, where AW is present. The exception here is the northeastern region of Iceland where we observe a clear warming trend of the ML (2010–2020). (v) We observe an “Atlantification” expressed as a northeastward progression of the  $\alpha$ -ocean state. This

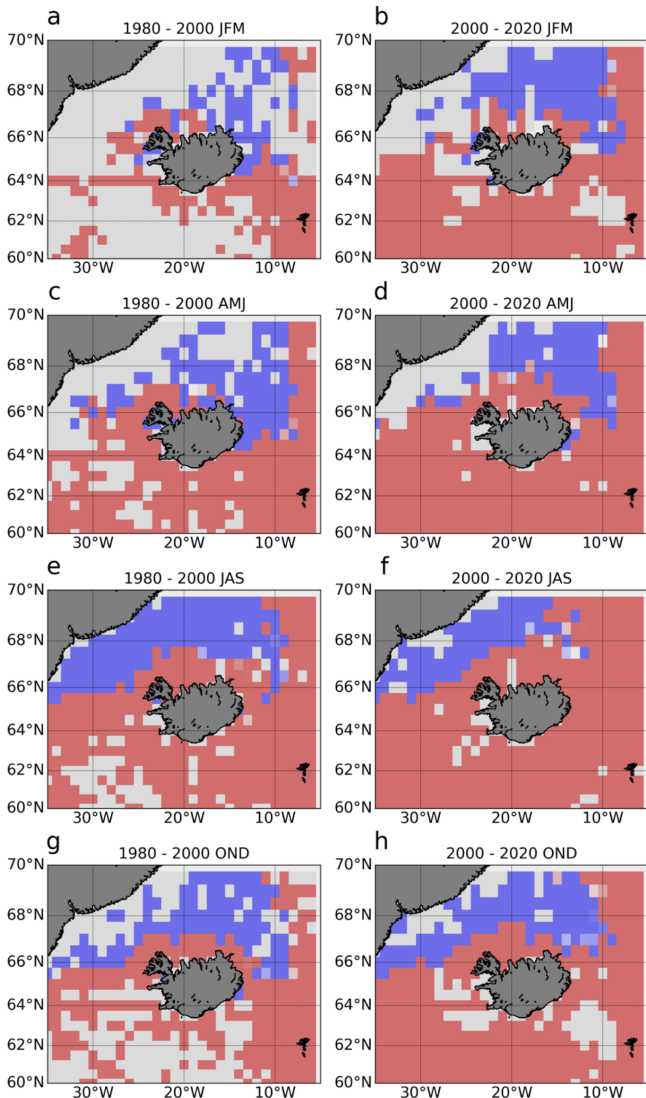


**Figure 9.** Mean upper 200 m spice frequency for the region of study showing the  $\alpha$ -ocean (red) and  $\beta$ -ocean (blue) regions for the periods of 1980–2000 and 2000–2020 and the four main seasons JFM (a, b), AMJ (c, d), JAS (e, f) and OND (g, h). The Brakstad et al. (2023) hydrographic dataset is used for this calculation.

progression will highlight the role of the northeastern area of Iceland as a convective zone where deep water could be formed and contribute to the NIJ.

**Code and data availability.** In situ data from the stations around Iceland were collected by the Marine and Fresh Water Research Institute (MFRI) of Iceland, provided by the SeaDataNet Pan-European infrastructure for ocean and marine data management (<https://cdi.seadatanet.org/search?step=00119900101>, last access: 22 November 2023).

**Supplement.** The supplement related to this article is available online at <https://doi.org/10.5194/os-22-1727-2026-supplement>.

**Author contributions.** Conceptualization, ARA, EP, and MDPH; methodology, ARA, EP and MDPH; software, ARA and AP; formal analysis, ARA, EP, TM, CdM and MDPH; investigation, ARA, EP and MDPH, AM; data acquisition, SRÓ and AM; data curation, SRÓ and AM; writing – original draft preparation, ARA, EP and MDPH; writing – review and editing, SRÓ, AM and SJ, TM; visualization, ARA and EP; project administration, SRÓ; funding acquisition, ARA and SRÓ. All authors have read and agreed to the published version of the manuscript.

**Competing interests.** The contact author has declared that none of the authors has any competing interests.

**Disclaimer.** Publisher's note: Copernicus Publications remains neutral with regard to jurisdictional claims made in the text, published maps, institutional affiliations, or any other geographical representation in this paper. The authors bear the ultimate responsibility for providing appropriate place names. Views expressed in the text are those of the authors and do not necessarily reflect the views of the publisher.

**Acknowledgements.** We are grateful for the invaluable cooperation we have had with the crews of the Icelandic research vessels Bjarni Sæmundsson and Árni Friðriksson and to the many people at the Marine Research Institute that have contributed to the hydrographic observations over the years. We are also grateful to the anonymous reviewers for their valuable feedback and constructive comments, which greatly improved the quality of this work. ARA and MDPH would like to dedicate this paper to the memory of Maria Casanova-Masjoan.

**Financial support.** ARA and CdM have been supported by HM Queen Margrethe II's and Vigdís Finnbogadóttir's Interdisciplinary Research Centre on Ocean, Climate and Society (ROCS) under grant no. 158-4223. Support for this work was also provided by the European Union's Horizon 2020 research and innovation programme under grant no. 727852, Blue-Action project (AM, SRO, and SJ). MDPH and ARA will like to acknowledge the DS-MIXSED international project funded by the Agencia Estatal de Investigación through the PCI 2024 call – project PCI2024-155022-2 and PCI2024-155084-2 and the Deutsche Forschungsgemeinschaft (DFG, German Research Foundation) – Projektnummer 541914507, and the FAR-DWO (PID2020-114322RB100) project from the Spanish Ministry of Research.

**Review statement.** This paper was edited by Agnieszka Beszczynska-Möller and reviewed by Sarah Gille and one anonymous referee.

## References

- Asthorsson, O. S., Valdimarsson, H., Gudmundsdottir, A., and Oskarsson, G. J.: Climate-related variations in the occurrence and distribution of mackerel (*Scomber scombrus*) in Icelandic waters, *ICES J. Mar. Sci.*, 69, 1289–1297, 2012.
- Athanase, M., Provost, C., Pérez-Hernández, M. D., Sennéchaël, N., Bertosio, C., Artana, C., Garric, G., and Lellouche, J. M.: Atlantic water modification north of Svalbard in the Mercator physical system from 2007 to 2020, *J. Geophys. Res.-Ocean.*, 125, e2020JC016463, <https://doi.org/10.1029/2020JC016463>, 2020.
- Bindoff, N. L., Cheung, W. W. L., Kairo, J. G., Arístegui, J., Gunder, V. A., Hallberg, R., Hilmi, N., Jiao, N., Karim, M. S., Levin, L., O'Donoghue, S., Purca Cuicapusa, S. R., Rinkevich, B., Suga, T., Tagliabue, A., and Williamson, P.: Changing Ocean, Marine Ecosystems, and Dependent Communities, In: IPCC Special Report on the Ocean and Cryosphere in a Changing Climate, edited by: Pörtner, H.-O., Roberts, D. C., Masson-Delmotte, V., Zhai, P., Tignor, M., Poloczanska, E., Mintenbeck, K., Alegría, A., Nicolai, M., Okem, A., Petzold, J., Rama, B., and Weyer, N. M., Cambridge University Press, Cambridge, UK and New York, NY, USA, 447–587, <https://doi.org/10.1017/9781009157964.007>, 2019.
- Brakstad, A.: Hydrographic and Geochemical Observations in the Nordic Seas Between 1950 and 2019, University of Bergen, <https://doi.org/10.21335/NMDC-1271328906>, 2023.
- Bersch, M.: North Atlantic Oscillation-induced changes of the upper layer circulation in the northern North Atlantic Ocean, *J. Geophys. Res.*, 107, 3156, <https://doi.org/10.1029/2001JC000901>, 2002.
- Campana, S. E., Stefansdottir, R. B., Jakobsdottir, K., and Solmundsson, J.: Shifting fish distributions in warming sub-Arctic oceans, *Sci. Rep.*, 10, 1–14, 2020.
- Carmack, E. C.: The alpha/beta ocean distinction: A perspective on freshwater fluxes, convection, nutrients and productivity in high-latitude seas, *Deep-Sea Res. Pt. II*, 54, 2578–2598, 2007.
- Casanova-Masjoan, M., Pérez-Hernández, M. D., Pickart, R. S., Valdimarsson, H., Ólafsdóttir, S. R., Macrander, A., Grisolia-Santos, D., Torres, D. J., Jónsson, S., Våge, K., and Lin, P.: Along-stream, seasonal, and interannual variability of the North Icelandic Irminger Current and East Icelandic Current around Iceland, *J. Geophys. Res.-Ocean.*, 125, e2020JC016283, <https://doi.org/10.1029/2020JC016283>, 2020.
- Cerfonteyn, M., Groben, R., Vaultot, D., Guðmundsson, K., Vannier, P., Pérez-Hernández, M. D. and Marteinson, V. þ.: The distribution and diversity of eukaryotic phytoplankton in the Icelandic marine environment, *Sci. Rep.*, 13, 8519, <https://doi.org/10.1038/s41598-023-35537-2>, 2023.
- Dai, A., Luo, D., Song, M., and Liu, J.: Arctic amplification is caused by sea-ice loss under increasing CO<sub>2</sub>, *Nat. Commun.*, 10, 1–13, 2019.
- de Boyer Montégut, C., Madec, G., Fischer, A. S., Lazar, A., and Iudicone, D.: Mixed layer depth over the global ocean: An examination of profile data and a profile-based climatology, *J. Geophys. Res.-Ocean.*, 109, <https://doi.org/10.1029/2004JC002378>, 2004.
- de Marez, C., Ruiz-Angulo, A., and Gula, J.: Mesoscale induced vertical fluxes over the Iceland-Faroe ridge, *Geophys. Res. Lett.*, 52, <https://doi.org/10.1029/2025GL115520>, 2025.
- de Marez, C., Vives, C. R., Portela, E., and Ruiz-Angulo, A.: Mesoscale ocean processes: The critical role of stratification in the Icelandic region, *J. Geophys. Res.-Ocean.*, 130, <https://doi.org/10.1029/2025JC022664>, 2025.
- Dickson, R., Lazier, J., Meincke, J., Rhines, P., and Swift, J.: Long-term coordinated changes in the convective activity of the North Atlantic, *Prog. Oceanogr.*, 38, [https://doi.org/10.1016/S0079-6611\(97\)00002-5](https://doi.org/10.1016/S0079-6611(97)00002-5), 1996.
- Feucher, C., Portela, E., Kolodziejczyk, N., and Thierry, V.: Subpolar gyre decadal variability explains the recent oxygenation in the Irminger Sea, *Commun. Earth Environ.*, 3, 279, <https://doi.org/10.1038/s43247-022-00570-y>, 2022.
- Foukal, N. P., Gelderloos, R., and Pickart, R. S.: A continuous pathway for fresh water along the east Greenland shelf, *Sci. Adv.*, 6, eabc4254, <https://doi.org/10.1126/sciadv.abc4254>, 2020.
- Fox-Kemper, B., Hewitt, H. T., Xiao, C., Aðalgeirsdóttir, G., Drifflou, S. S., Edwards, T. L., Golledge, N. R., Hemer, M., Kopp, R. E., Krinner, G., Mix, A., Notz, D., Nowicki, S., Nurhati, I. S., Ruiz, L., Sallée, J.-B., Slangen, A. B. A., and Yu, Y.: Ocean, Cryosphere and Sea Level Change, in: Climate Change 2021: The Physical Science Basis. Contribution of Working Group I to the Sixth Assessment Report of the Intergovernmental Panel on Climate Change, edited by: Masson-Delmotte, V., Zhai, P., Pirani, A., Connors, S. L., Péan, C., Berger, S., Caud, N., Chen, Y., Goldfarb, L., Gomis, M. I., Huang, M., Leitzell, K., Lonnoy, E., Matthews, J. B. R., Maycock, T. K., Waterfield, T., Yelekçi, O., Yu, R., and Zhou, B.: Cambridge University Press, Cambridge, United Kingdom and New York, NY, USA, 1211–1362, <https://doi.org/10.1017/9781009157896.011>, 2021.
- Gjelstrup, C. V. B., Sejr, M. K., de Steur, L., Christiansen, J. S., Granskog, M. A., Koch, B. P., Møller, E. F., Winding, M. H. S., and Stedmon, C. A.: Vertical redistribution of principle water masses on the northeast Greenland Shelf, *Nat. Commun.*, 13, <https://doi.org/10.1038/s41467-022-35413-z>, 2022.
- Hansen, B. and Østerhus, S.: North Atlantic–Nordic Seas exchanges, *Prog. Oceanogr.*, 45, 109–208, 2000.
- Hansen, B., Larsen, K. M. H., Hátún, H., Olsen, S. M., Gierisch, A. M. U., Østerhus, S., and Ólafsdóttir, S. R.: The Iceland–Faroe warm-water flow towards the Arctic estimated from satellite altimetry and in situ observations, *Ocean Sci.*, 19, 1225–1252, <https://doi.org/10.5194/os-19-1225-2023>, 2023.
- Harden, B.E., Pickart, R.S., Valdimarsson, H., Våge, K., de Steur, L., Richards, C., Bahr, F., Torres, D., Børve, E., Jónsson, S. and Macrander, A.: Upstream sources of the Denmark Strait overflow: Observations from a high-resolution mooring array, *Deep-Sea Res. Pt. I*, 112, 94–112, 2016.
- Hátún, H. and Chafik, L.: On the recent ambiguity of the North Atlantic Subpolar Gyre Index, *J. Geophys. Res.-Ocean.*, 123, 5072–5076, 2018.
- Hátún, H., Chafik, L., and Larsen, K. M. H.: The Norwegian Sea Gyre – a regulator of Iceland-Scotland Ridge exchanges, *Front. Mar. Sci.*, 8, 1001, <https://doi.org/10.3389/fmars.2021.694614>, 2021.
- Håvik, L., Pickart, R. S., Våge, K., Torres, D., Thurnherr, A. M., Beszczynska-Möller, A., Walczowski, W., and Von Appen, W. J.: Evolution of the East Greenland Current from Fram Strait to Denmark Strait: Synoptic measurements from summer 2012, *J. Geophys. Res.-Ocean.*, 122, 1974–1994, 2017.

- Hersbach, H., Bell, B., Berrisford, P., Hirahara, S., Horányi, A., Muñoz-Sabater, J., Nicolas, J., Peubey, C., Radu, R., Schepers, D., and Simmons, A.: The ERA5 global reanalysis, *Q. J. R. Meteorol. Soc.*, 146, 1999–2049, <https://doi.org/10.1002/qj.3803>, 2020.
- Holliday, N. P., Bersch, M., Berx, B., Chafik, L., Cunningham, S., Florindo-López, C., Hátún, H., Johns, W., Josey, S. A., Larsen, K. M. H., and Mulet, S.: Ocean circulation causes the largest freshening event for 120 years in eastern subpolar North Atlantic, *Nat. Commun.*, 11, 2020.
- Holt, J., Schrum, C., Cannaby, H., Daewel, U., Allen, I., Artioli, Y., Bopp, L., Butenschon, M., Fach, B. A., Harle, J., and Pushpadas, D.: Potential impacts of climate change on the primary production of regional seas: A comparative analysis of five European seas, *Prog. Oceanogr.*, 140, 91–115, 2016.
- Holte, J., Talley, L. D., Gilson, J., and Roemmich, D.: An Argo mixed layer climatology and database, *Geophys. Res. Lett.*, 44, 5618–5626, 2017.
- Huang, J., Pickart, R. S., Chen, Z., and Huang, R. X.: Role of air-sea heat flux on the transformation of Atlantic Water encircling the Nordic Seas, *Nat. Commun.*, 14, <https://doi.org/10.1038/s41467-023-35889-3>, 2023.
- Hurrell, J. W.: Decadal trends in the North Atlantic Oscillation: Regional temperatures and precipitation, *Science*, 269, 5224, <https://doi.org/10.1126/science.269.5224.676>, 1995.
- Jónsson, S.: The circulation in the northern part of the Denmark Strait and its variability, *ICES CM*, 50, <https://doi.org/10.17895/ices.pub.25637283>, 1999.
- Jónsson, S. and Briem, J.: Flow of Atlantic water west of Iceland and onto the North Icelandic shelf, *ICES Marine Science Symposia*, 219, 326–328, <https://doi.org/10.17895/ices.pub.19271852>, 2003.
- Jónsson, S. and Valdimarsson, H.: Water mass transport variability to the North Icelandic shelf, 1994–2010, *ICES J. Mar. Sci.*, 69, 809–815, <https://doi.org/10.1093/icesjms/fss024>, 2012.
- Kohler, J., Serra, N., Bryan, F. O., Johnson, B. K., and Stammer, D.: Mechanisms of mixed-layer salinity seasonal variability in the Indian Ocean, *J. Geophys. Res.-Ocean.*, 123, 466–496, 2018.
- Li, G., Cheng, L., Zhu, J., Trenberth, K. E., Mann, M. E., and Abraham, J. P.: Increasing ocean stratification over the past half-century, *Nat. Clim. Chang.*, 10, 1116–1123, 2020.
- Lin, P., Pickart, R. S., Jochumsen, K., Moore, G. W. K., Valdimarsson, H., Fristedt, T., and Pratt, L. J.: Kinematic structure and dynamics of the Denmark Strait overflow from ship-based observations, *J. Phys. Oceanogr.*, 50, 2020.
- Liu, C., Liang, X., Chambers, D. P., and Ponte, R. M.: Global patterns of spatial and temporal variability in salinity from multiple gridded Argo products, *J. Clim.*, 33, 8751–8766, 2020.
- Logemann, K., Ólafsson, J., Snorrason, Á., Valdimarsson, H., and Marteinsdóttir, G.: The circulation of Icelandic waters – a modelling study, *Ocean Sci.*, 9, 931–955, <https://doi.org/10.5194/os-9-931-2013>, 2013.
- Lozier, M. S., Li, F., Bacon, S., Bahr, F., Bower, A.S., Cunningham, S. A., de Jong, M. F., de Steur, L., deYoung, B., Fischer, J., and Gary, S. F.: A sea change in our view of overturning in the subpolar North Atlantic, *Science*, 363, 516–521, 2019.
- Macrander, A., Valdimarsson, H., and Jonsson, S.: Improved transport estimate of the East Icelandic Current 2002–2012, *J. Geophys. Res.-Ocean.*, 119, 3407–3424, 2014.
- Mastropole, D., Pickart, R. S., Valdimarsson, H., Våge, K., Jochumsen, K., and Girton, J.: On the hydrography of Denmark Strait, *J. Geophys. Res.-Ocean.*, 122, 306–321, 2017.
- Mauritzen, C.: Production of dense overflow waters feeding the North Atlantic across the Greenland-Scotland Ridge, Part 1: Evidence for a revised circulation scheme, *Deep-Sea Res. Pt. I*, 43, 769–806, 1996.
- Moore, G. W. K., Våge, K., Pickart, R. S., and Renfrew, I. A.: Decreasing intensity of open-ocean convection in the Greenland and Iceland seas, *Nat. Clim. Change*, 5, 877–882, 2015.
- Ólafsson, J.: Winter mixed layer nutrients in the Irminger and Iceland seas, *ICES Mar. Sci. Symp.*, 219, 329–332, 2003.
- Ólafsdóttir, A. H., Utne, K. R., Jacobsen, J. A., Jansen, T., Óskarsson, G. J., Nøttestad, L., Elvarsson, B. P., Broms, C., and Slotte, A.: Geographical expansion of Northeast Atlantic mackerel (*Scomber scombrus*) in the Nordic Seas from 2007 to 2016 was primarily driven by stock size and constrained by low temperatures, *Deep-Sea Res. Pt. II*, 159, 152–168, 2019.
- Østerhus, S., Woodgate, R., Valdimarsson, H., Turrell, B., de Steur, L., Quadfasel, D., Olsen, S. M., Moritz, M., Lee, C. M., Larsen, K. M. H., Jónsson, S., Johnson, C., Jochumsen, K., Hansen, B., Curry, B., Cunningham, S., and Berx, B.: Arctic Mediterranean exchanges: a consistent volume budget and trends in transports from two decades of observations, *Ocean Sci.*, 15, 379–399, <https://doi.org/10.5194/os-15-379-2019>, 2019.
- Pérez-Hernández, M. D., Pickart, R. S., Torres, D. J., Bahr, F., Sundfjord, A., Ingvaldsen, R., Renner, A. H., Beszczynska-Möller, A., von Appen, W. J., and Pavlov, V.: Structure, transport, and seasonality of the Atlantic Water boundary current north of Svalbard: Results from a yearlong mooring array, *J. Geophys. Res.-Ocean.*, 124, 1679–1698, 2019.
- Petit, T., Lozier, M. S., Josey, S. A., and Cunningham, S. A.: Atlantic deep water formation occurs primarily in the Iceland Basin and Irminger Sea by local buoyancy forcing, *Geophys. Res. Lett.*, 47, e2020GL091028, <https://doi.org/10.1029/2020GL091028>, 2020.
- Petit, T., Lozier, M. S., Josey, S. A., and Cunningham, S. A.: Role of air–sea fluxes and ocean surface density in the production of deep waters in the eastern subpolar gyre of the North Atlantic, *Ocean Sci.*, 17, 1353–1365, <https://doi.org/10.5194/os-17-1353-2021>, 2021.
- Piron, A., Thierry, V., Mercier, H., and Caniaux, G.: Argo float observations of basin-scale deep convection in the Irminger Sea during winter 2011–2012, *Deep-Sea Res. Pt. I*, 109, 76–90, 2016.
- Polyakov, I. V., Pnyushkov, A. V., Alkire, M. B., Ashik, I. M., Baumann, T. M., Carmack, E. C., Goszczko, I., Guthrie, J., Ivanov, V. V., Kanzow, T., and Krishfield, R.: Greater role for Atlantic inflows on sea-ice loss in the Eurasian Basin of the Arctic Ocean, *Science*, 356, 285–291, 2017.
- Polyakov, I. V., Rippeth, T. P., Fer, I., Alkire, M. B., Baumann, T. M., Carmack, E. C., Ingvaldsen, R., Ivanov, V. V., Janout, M., Lind, S., and Padman, L.: Weakening of cold halocline layer exposes sea ice to oceanic heat in the eastern Arctic Ocean, *J. Clim.*, 33, 8107–8123, 2020.
- Price, J. F., Weller, R. A., and Pinkel, R.: Diurnal cycling – Observations and models of the upper ocean response to diurnal heating, cooling, and wind mixing, *J. Geophys. Res.-Ocean.*, 91, 8411–8427, 1986.

- Renfrew, I. A., Pickart, R. S., Våge, K., Moore, G. W., Bracegirdle, T. J., Elvidge, A. D., Jeansson, E., Lachlan-Cope, T., McRaven, L. T., Papritz, L., and Reuder, J.: The Iceland Greenland Seas Project, *Bull. Am. Meteorol. Soc.*, 100, 1795–1817, 2019.
- Richardson, K. and Bendtsen, J.: Distinct seasonal primary production patterns in the sub-polar gyre and surrounding seas, *Front. Mar. Sci.*, <https://doi.org/10.3389/fmars.2021.785685>, 2021.
- Rudels, B., Björk, G., Nilsson, J., Winsor, P., Lake, I., and Nohr, C.: The interaction between waters from the Arctic Ocean and the Nordic Seas north of Fram Strait and along the East Greenland Current: Results from the Arctic Ocean-02 Oden expedition, *J. Mar. Syst.*, 55, 1–30, 2005.
- Sallée, J. B., Pellichero, V., Akhoudas, C., Pauthenet, E., Vignes, L., Schmidtko, S., Garabato, A. N., Sutherland, P., and Kuusela, M.: Summertime increases in upper-ocean stratification and mixed-layer depth, *Nature*, 591, 592–598, <https://doi.org/10.1038/s41586-021-03303-x>, 2021.
- Sarafanov, A.: On the effect of the North Atlantic Oscillation on temperature and salinity of the subpolar North Atlantic intermediate and deep waters, *ICES J. Mar. Sci.*, 66, 1448–1454, 2009.
- Semper, S., Våge, K., Pickart, R. S., Valdimarsson, H., Torres, D. J., and Jónsson, S.: The emergence of the North Icelandic Jet and its evolution from Northeast Iceland to Denmark Strait, *J. Phys. Oceanogr.*, 49, 2499–2521, 2019.
- Shepherd, J. G., Brewer, P. G., Oschlies, A., and Watson, A. J.: Ocean ventilation and deoxygenation in a warming world: Introduction and overview, *Philos. Trans. A Math. Phys. Eng. Sci.*, 375, <https://doi.org/10.1098/rsta.2017.0240>, 2017.
- Skyllingstad, E. D., Samelson, R. M., Simmons, H., Laurent, L. S., Merrifield, S., Klenz, T., and Centurioni, L.: Boundary layer energetics of rapid wind and wave forced mixing events, *J. Phys. Oceanogr.*, 53, 1887–1900, 2023.
- Stewart, K. D. and Haine, T. W.: Thermobaricity in the transition zones between alpha and beta oceans, *J. Phys. Oceanogr.*, 46, 1805–1821, 2016.
- Strehl, A.-M., Våge, K., Merdrud, S. L. H., and Barreyre, T.: A 70-year perspective on water-mass transformation in the Greenland Sea: From thermobaric to thermal convection, *Prog. Oceanogr.*, 227, 103304, <https://doi.org/10.1016/j.pocean.2024.103304>, 2024.
- Tesdal, J.-E., Abernathey, R. P., Goes, J. I., Gordon, A. L., and Haine, T. W.: Salinity trends within the upper layers of the sub-polar North Atlantic, *J. Clim.*, 31, 2675–2698, 2018.
- Valdimarsson, H., Astthórsson, O. S., and Pálsson, J.: Hydrographic variability in Icelandic waters during recent decades and related changes in distribution of some fish species, *ICES J. Mar. Sci.*, 69, 816–825, <https://doi.org/10.1093/icesjms/fss027>, 2012.
- Våge, K., Pickart, R. S., Moore, G., and Ribergaard, M. H.: Winter mixed layer development in the central Irminger Sea: The effect of strong, intermittent wind events, *J. Phys. Oceanogr.*, 38, 541–565, 2008.
- Våge, K., Pickart, R. S., Spall, M. A., Valdimarsson, H., Jónsson, S., Torres, D. J., Østerhus, S., and Eldevik, T.: Significant role of the North Icelandic Jet in the formation of Denmark Strait Overflow Water, *Nat. Geosci.*, 4, 723–727, 2011.
- Våge, K., Pickart, R. S., Spall, M. A., Moore, G. W. K., Valdimarsson, H., Torres, D. J., Erofeeva, S. Y., and Nilsen, J. E. Ø.: Revised circulation scheme north of the Denmark Strait, *Deep-Sea Res. Pt. I*, 79, 20–39, 2013.
- Våge, K., Moore, G. W. K., Jónsson, S., and Valdimarsson, H.: Water mass transformation in the Iceland Sea, *Deep-Sea Res. Pt. I*, 101, 98–109, 2015.
- Våge, K., Papritz, L., Havik, L., Spall, M. A., and Moore, G. W. K.: Ocean convection linked to the recent ice edge retreat along East Greenland, *Nat. Commun.*, 9, 1–8, 2018.
- Våge, K., Semper, S., Valdimarsson, H., Jónsson, S., Pickart, R. S., and Moore, G. W. K.: Water mass transformation in the Iceland Sea: Contrasting two winters separated by four decades, *Deep-Sea Res. Pt. I*, 186, 103824, <https://doi.org/10.1016/j.dsr.2015.04.001>, 2022.
- Whitney, M. M.: Icelandic riverine freshwater distribution, offshore export, and alongshelf connectivity, *Estuar. Coast. Shelf Sci.*, 319, 109266, <https://doi.org/10.1016/j.ecss.2025.109266>, 2025.
- Yamaguchi, R. and Suga, T.: Trend and variability in global upper-ocean stratification since the 1960s, *J. Geophys. Res.-Ocean.*, 124, 8933–8948, 2019.
- Zhai, L., Gudmundsson, K., Miller, P., Peng, W., Guðfinnsson, H., Debes, H., Hátún, H., White III, G. N., Walls, R. H., Sathyendranath, S., and Platt, T.: Phytoplankton phenology and production around Iceland and Faroes, *Cont. Shelf Res.*, 37, 2012.